Scientific Research Publishing

Open Journal of Geology, 2024, 14, 723-745
https://www.scirp.org/journal/ojg
ISSN Online: 2161-7589
ISSN Print: 2161-7570

Hydrocarbon Potential of the Triassic-Jurassic Sediments in Southeast Sulawesi, Indonesia, Based on Lithofacies and Geochemical Analysis

Muhammad Sulhuzair Burhanuddin[1,2], Shun Chiyonobu[1], Takuto Ando[1], Anggi Yusriani[3], Ratna Husain[2], Suryawan Asfar[4]

[1]Graduate School of International Resources Sciences, Akita University, Akita, Japan
[2]Geological Department of Hasanuddin University, Makassar, Indonesia
[3]Geoservices Laboratory, South Jakarta, Indonesia
[4]Geological Department of Haluoleo University, Kendari, Indonesia
Email: muhammadsulhuzair@gmail.com

How to cite this paper: Burhanuddin, M.S., Chiyonobu, S., Ando, T., Yusriani, A., Husain, R. and Asfar, S. (2024) Hydrocarbon Potential of the Triassic-Jurassic Sediments in Southeast Sulawesi, Indonesia, Based on Lithofacies and Geochemical Analysis. *Open Journal of Geology*, **14**, 723-745.
https://doi.org/10.4236/ojg.2024.148031

Received: July 17, 2024
Accepted: August 6, 2024
Published: August 9, 2024

Abstract

Triassic-Jurassic carbonates widely distributed in Eastern Indonesia are believed as oils source rock. The Mesozoic Tokala Formation exhibit source rock potential, as evidenced by high contents of organic matter. Recent exploration has been conducted in southeastern Sulawesi, targeting the Mesozoic intervals. Therefore, in this study, we attempted to determine source rock potential of Tokala Formation outcropped in southeastern Sulawesi area and its capability to generate hydrocarbon. Five distinct lithofacies were delineated, emphasizing lithological and mineralogical features: foraminifera wackestone (FW), lime mudstone (LM), massive bioturbated calcareous-argillaceous shale (MBCAS), weakly laminated argillaceous-calcareous shale (WLACS), and strongly laminated calcareous-argillaceous shale (SLCAS). Subsequent analyses showed that carbonate-rich samples (FW and LM facies, >50% CaO) had poor source rock potential. Conversely, shale facies with moderate carbonate content (WLACS, MBCAS, and SLCAS, 15% - 50% CaO) had good to excellent source rock characteristics, qualifying them as preferable source rock. In addition, levels of SiO_2 and Al_2O_3 should not be neglected, as these constituents play important roles in clay mineral adsorption. Laminated shale facies with moderate CaO content tended to be more promising as source rock than bioturbated facies. The shale facies of Tokala Formation indicate prospective source rock horizon.

Keywords

Source Rock, Triassic-Jurassic, Source Rock Lithofacies, Southeastern Sulawesi,

Tokala Formation

1. Introduction

Indonesia has many petroleum-bearing sedimentary basins, classified as producing, discovering, prospective, and unexplored basins [1]. However, exploration activities in Indonesia mainly focused on the western part, in which most of the producing basin situated in western Indonesia. In contrast, in the eastern part, most of the basins could be categorized as frontier area due to several reasons. First, tectonically, eastern part of Indonesia is quite complex compared with the western part of Indonesia, which implies to the petroleum system, particularly generation and migration subsystem [2]. Second, the source rock is poorly understood due to the lack of geological database (limited outcrop and remote area), and scarces well and seismic data.

Despite of that, several authors have classified three main souce rock groups in the eastern Indonesia from main producing basins [3]-[5]. These groups are the Mesozoic carbonate in Seram Basin [6] [7]; Buton Basin [8] [9], Mesozoic marine shale in Timor [10], Paleogene and Neogene marine shales in Salawati Basin [11] [12]; Bintuni Basin [13] [14]; and Banggai Basin [15]. Southeast Sulawesi, however, located between two petroliferous area, which are Banggai area (mostly gas production) in the north and Buton area (asphalt mining) in the south. While exploration activities in Northern Southeast Sulawesi was not massive compared to the neighboring area (productive basins), numerous hydrocarbon manifestation have been reported [16] [17]. The Triassic Jurassic Tokala Fromation have been reported to have potential as a source rock in Tomori Basin [18], however detail characteristics are required, as the Tokala Formation also widely distributed in Southeast Sulawesi [19] [20].

The objective of this present study is to characterize the geochemical attributes and assess the hydrocarbon potential of outcropping exposures of the Tokala Formation in Southeast Sulawesi through an integrated multidisciplinary analysis. Rather than relying solely on conventional geological techniques alone, we would like to present a comprehensive attempt combining classical geological approach, such as field mapping and petrography analysis, with the most common practice in petroleum studies, such as detailed geochemistry analysis to study about the petroleum potential from outcrop samples of Tokala Formation in Southeast Sulawesi area.

2. Geological Settings

Sulawesi Island is divided into four tectonic provinces [20] separated by complex structures from west to east, *i.e.*, a magmatic arc, central metamorphic block, ophiolite belt, and Australian-derived microcontinent. However, the borders between each tectonic province are unclear; for example, some pre-Tertiary

sedimentary rocks occurred as small blocks in the ophiolite belt province. Our research area is situated in southeastern Sulawesi (**Figure 1**), where part of the microcontinent is bounded by two major strike-slip faults, the Matano Fault in the north and the Lawanopo Fault in the southern part [20] [21] [22].

Southeastern Sulawesi was formed in multiple tectonic stages, from the breakup of Gondwana to the collision of microcontinents in the Sundaland margin, resulting in complex pre-Tertiary to Tertiary stratigraphic variation (**Figure 2**; [20]-[23]). The southeastern Sulawesi fragment [24] rifted from Gondwana (Western Australia) from the Early Permian to the Triassic. During the syn-rift stage, basin filling was dominated by the deposition of terrestrial to fluvio-deltaic sediments represented by the Meluhu Formation. Later, marine incursion resulted in carbonate development in the basinal area, while siliciclastic deposition continued in the west (**Figure 2**; [20]). This carbonate interval, referred to as the Tokala Formation [20] [21] [25], was deposited on the carbonate platform with intertidal to carbonate reef facies, while carbonate reef was drowned due to rapid subsidence in the upper part [20]. This Triassic-Jurassic carbonate may be correlated with other carbonates in eastern Indonesia, such as the Manusela and Saman-Saman formations in the Seram basin [26] [27] and Winto Formation in the Buton basin [8] [20]. Rifting continued until a breakup event marked by regional unconformable boundaries as a result of major uplift.

After the breakup event, northward-oriented drifting of the microcontinent occurred from the Cretaceous through the Early Cenozoic [24]. During this drifting stage, the basin was far from the sediment source, resulting in dominant carbonate deposition, as represented by two carbonate formations, the Cretaceous Matano and Paleogene Tampakura formations (**Figure 2**; [20]-[22]).

The drifting period was terminated by Early Miocene collision of the Banggai-Sula microcontinent, resulting in major uplift of the pre-Tertiary interval, which was the provenance of later deposition through the Neogene (**Figure 2**; [22] [28]). These syn- to post-orogenic deposits were defined [28] and references therein] into the Early Miocene Bungku Formation, Late Miocene Pandua Formation, Miocene-Pleistocene Langkowala Formation, and Pliocene Eemoiko Formation. The youngest formations in the area are the Quaternary clastic Buara Formation and carbonate Alangga Formation [28]. This study focused on carbonate intervals of the Tokala Formation, which are distributed extensively throughout the southeastern Sulawesi region. However, as age data were not available, the formation was assigned based on the regional lithostratigraphy [20].

3. Materials and Methods

To provide a more detailed description, the materials in this study refer to all the samples and resulting datasets obtained and generated after conducting various analyses. The methods pertain to all the laboratory analyses, including analytical techniques such as field observation, petrographic observation, X-ray fluorescence

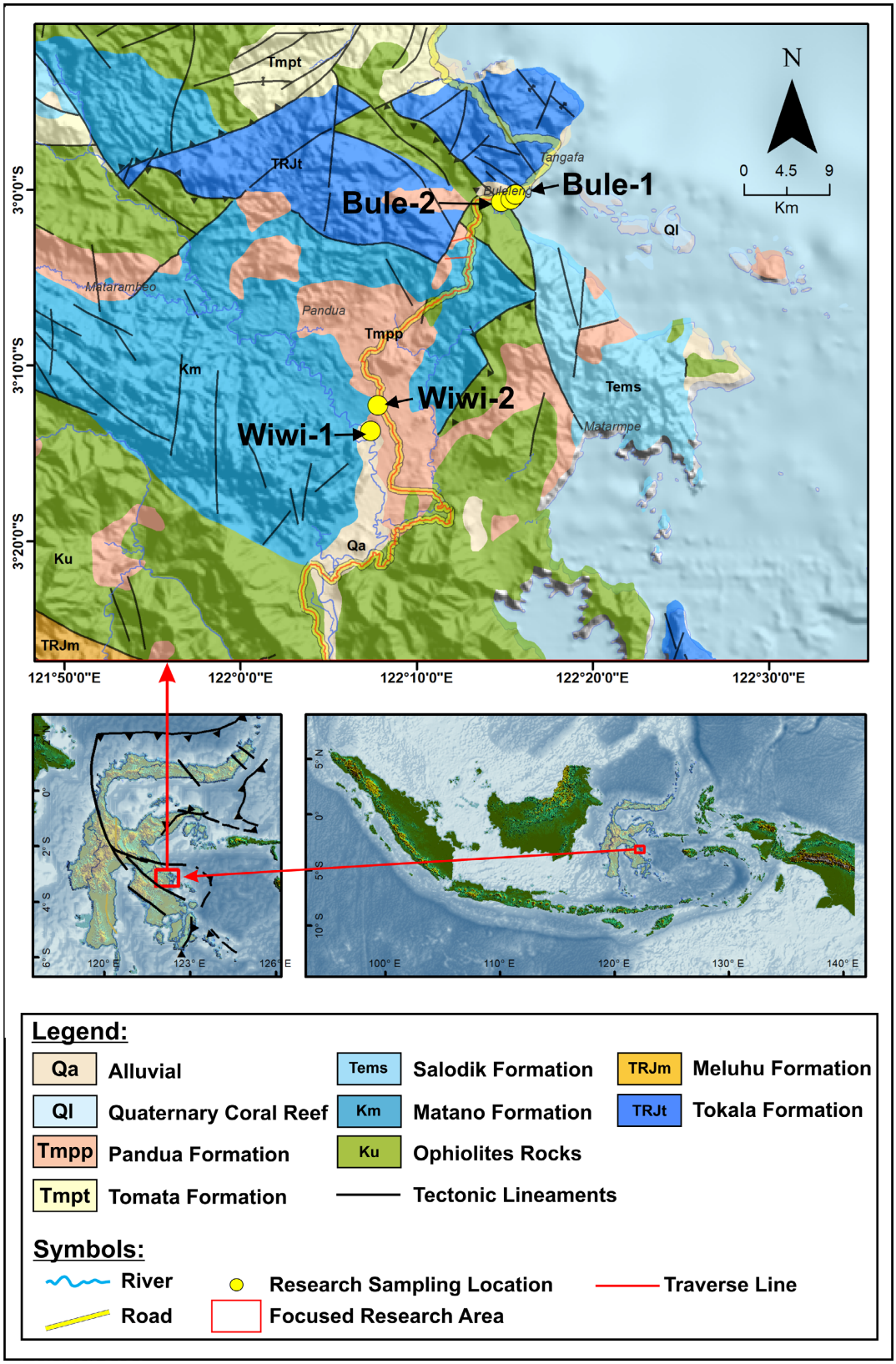

Figure 1. Regional geological map of southeastern Sulawesi [21] [22]. Red square indicates our research area. Geological surveys focused on Mesozoic carbonate interval. Hydrocarbons sampled from outcrops for biomarker analysis are noted.

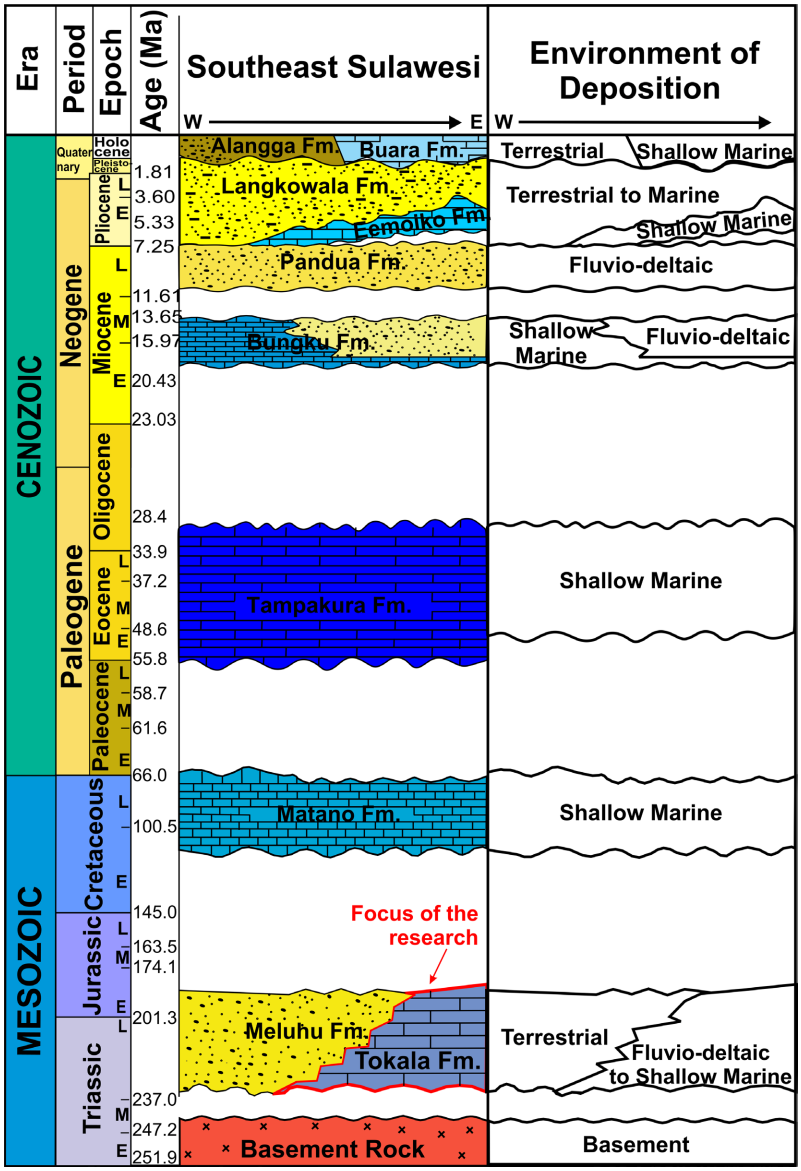

Figure 2. Regional tectonostratigraphy of southeastern Sulawesi, with the depositional environment (after [21] [22]). This research focused on Mesozoic carbonate intervals, including the Triassic-Jurassic Tokala Formation (after [20] [21]).

(XRF), and organic geochemistry analysis, performed using specific instruments.

3.1. Field Observation and Sampling

Geological field observations were conducted in North Konawe and South Bungku, southeastern Sulawesi, in four stratigraphic sections from south to north: Wiwi-1, Wiwi-2, Bule-1, and Bule-2 (**Figure 1**). Based on a previous survey by the Indonesia Geological Agency [21], lithologies traversed in all sections belonged to the Tokala Formation. Because no age data were available and biostratigraphic analysis was not the main focus of this study, the assignment of the formations was later validated based on correlations between lithological char-

acteristics and regional lithostratigraphy [19]-[21]. A total of 72 rock samples were collected from shale and limestone outcrops along road cuts. These samples were considered fresh because the outcrops were excavated to a thickness of at least 15 cm prior to sampling. Two samples showing oil stains was also acquired from limestone in the Bule-1 and Bule-2 sections (**Figure 1**). To ensure preservation, all samples were stored in well-sealed plastic bags, and the oil-stained rock was wrapped with aluminum foil to avoid contamination [29].

3.2. Petrographic Analysis

A total of 27 samples (19 shale, 8 limestone) selected from all sections were used for petrographic analysis to obtain detailed lithological descriptions. Prior to preparation, shale was hardened with epoxy solution (resin and catalyst) and left for 12 h to avoid internal breakup, because the lithology was too friable for primary cutting. After primary cutting, shale and limestone chunks were polished sequentially with mesh #350, #800, #1000, #2000, and #3000, and attached to glass slides. Secondary cutting was performed to thin attached samples to a thickness of ca. 1 - 2 mm, and a Prepa-Lap cutter (Maruto Instrument, Fukuoka, Japan) equivalent to #600 mesh powder, was utilized to grind thick blocks down to a thickness of ca. 30 μm. Finally, the samples were polished sequentially with powder from mesh #1000, #2000, #3000, and #6000. These petrographic slides were observed under a microscope with transmitted and reflected light (H600L; Nikon, Tokyo, Japan).

3.3. X-Ray Fluorescence (XRF) Analysis

A total of 49 representative samples (43 shale, 6 limestone) from all sections were subjected to XRF analysis (ZXS Primus II XRF; Rigaku, Tokyo, Japan) to determine the content of major oxides (SiO_2, TiO_2, Al_2O_3, Fe_2O_3, MnO, MgO, CaO, K_2O, and P_2O_5) and some trace elements (Ba, Cr, Cu, Nb, Ni, Pb, Rb, S, Sr, V, Y, Zn, and Zr). Prior to analysis, samples were pulverized to obtain 5 - 6 g of homogeneous powder, which was carefully placed within the assigned pellet rings. The sample powders were compressed using a flat disk to obtain appropriate pellet samples, as described in detail elsewhere [30].

3.4. Bulk Organic Geochemistry

Source rock characteristics were evaluated by pyrolysis to determine the bulk organic geochemical compositions of 72 samples (40 shales, 10 mudstones, and 22 limestones) using the Rock-Eval 6 apparatus (Vinci Technologies, Nanterre, France). These samples were ground into #300 - #400 mesh powder samples (clay size), of which 0.6 - 0.7 g was placed in crucibles for later analysis, as described previously (Lafargue *et al.*, 1998; Behar *et al.*, 2001). Parameters acquired in Rock-Eval analysis included total organic carbon (TOC); the amounts of free hydrocarbons detected in the sample (S1), and generated via the thermal cracking of nonvolatile organic matter (S2); the amount of carbon dioxide (CO_2) gen-

erated through kerogen pyrolysis (S3); and Tmax.

4. Results

4.1. Outcrop and Micro-Scale Lithofacies Characteristics

From the south section, the stratigraphic interval of the Tokala Formation consisted of intercalated limestone and shale, with limestone beds predominating in the Wiwi-1 section (Figure 3). The limestone and shale were well stratified with a sharp contact (Figure 4(A), Figure 4(B)), where the Limestone was light gray, matrix-supported, moderately sorted, and massive, with each layer ranging in thickness from 32 to 50 cm (Figure 4(D)). Under microscopic observation, the limestone was composed of skeletal grains, mostly foraminifera followed by mollusk grains, in a micritic matrix; therefore, the lithology was assigned as foraminifera wackestone (FW) facies.

Foraminifera were diverse, with elongated, oval, and circular shapes. Thin shale layers (5 - 12 cm) intercalated with wackestone were matrix-supported, intensively bioturbated, composed of carbonate grains within argillaceous matrix and occasional carbonaceous layers (Figure 4(C), Figure 4(E), Figure 4(I)). Carbonate grains were predominantly composed of skeletal fragments derived from foraminifera and mollusks ranging in size from 0.15 to 1.1 mm. Compared to the limestone, skeletal grains in the shale layers tended to be homogeneous. Notably, almost all original structures of the skeletal fragments had already been destroyed by extensive diagenesis, specifically neomorphism, as large calcite crystals grew within shells (Figures 4(F)-(H)). Significant concentrations of

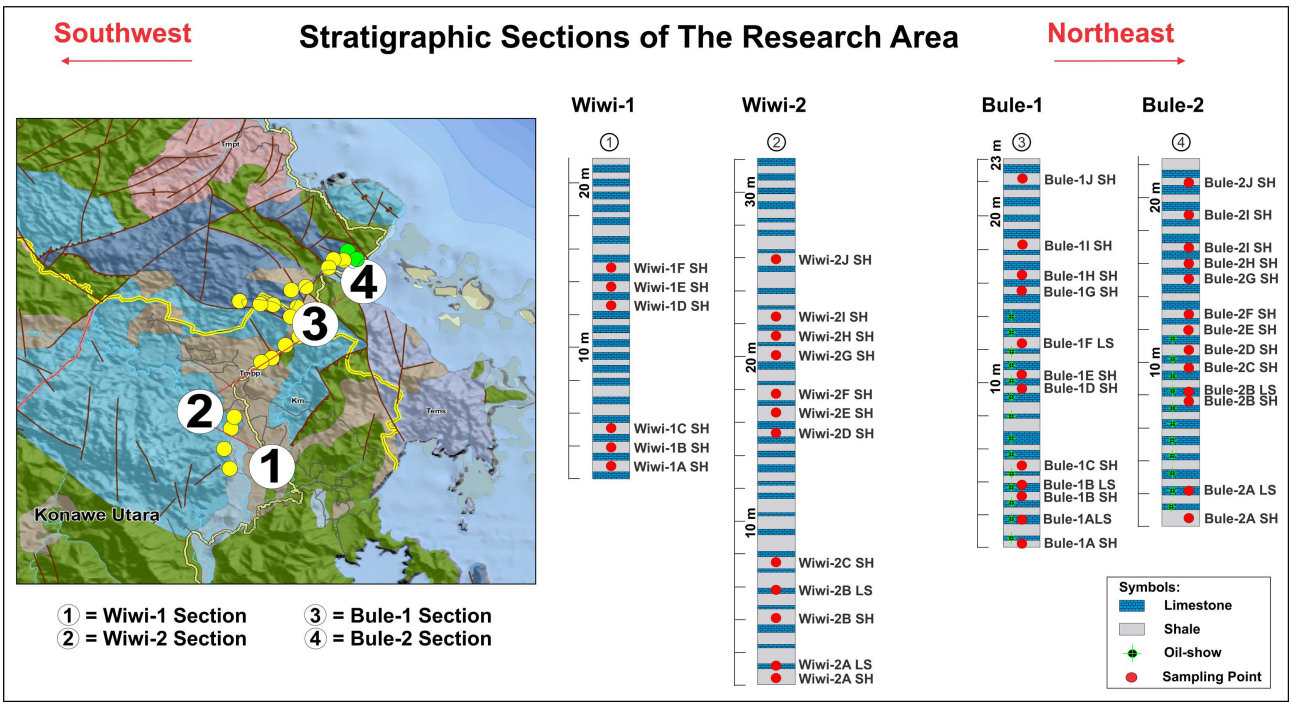

Figure 3. Stratigraphic succession of the traversed Triassic-Jurassic Tokala Formation. The stratigraphic section comprised four sections distributed over a 116-km distance from south to north: Wiwi-1, Wiwi-2, Bule-1, and Bule-2.

amorphous organic matter (AOM) and structured organic matter (SOM) were observed in the size range of 0.025 - 0.060 mm (Figure 4(I)). This organic matter was dispersed throughout the matrix, but occasionally occurred as laminas (Figure 4(E), Figure 4(F)). Another significant feature observed during macroscopic examination was the occurrence of bioturbation within the shale layer (Figure 4(C)). Later, shale in the Wiwi-1 section was assigned as massive bioturbated shale (MBS) facies.

Another shale/limestone alternation of the Tokala Formation was outcropped in the Wiwi-2 section, but in contrast to that described in the previous section, this alternation was dominated by shale approximately 42 m thick (Figure 5(A), Figure 5(C)). The limestone was poorly stratified and contact between these lithologies was unclear as the layer tended to be discontinuous. Interestingly, deformation was observed, where the more brittle limestone blocks showed signs of fracture and the underlying shale layers tended to be bent due to its ductility (Figure 5(D)). Shales were dark gray and could be considered massive based on field observations, but tended to have weak (irregularly sinuous) lamination (Figure 5(F), Figure 5(G)).

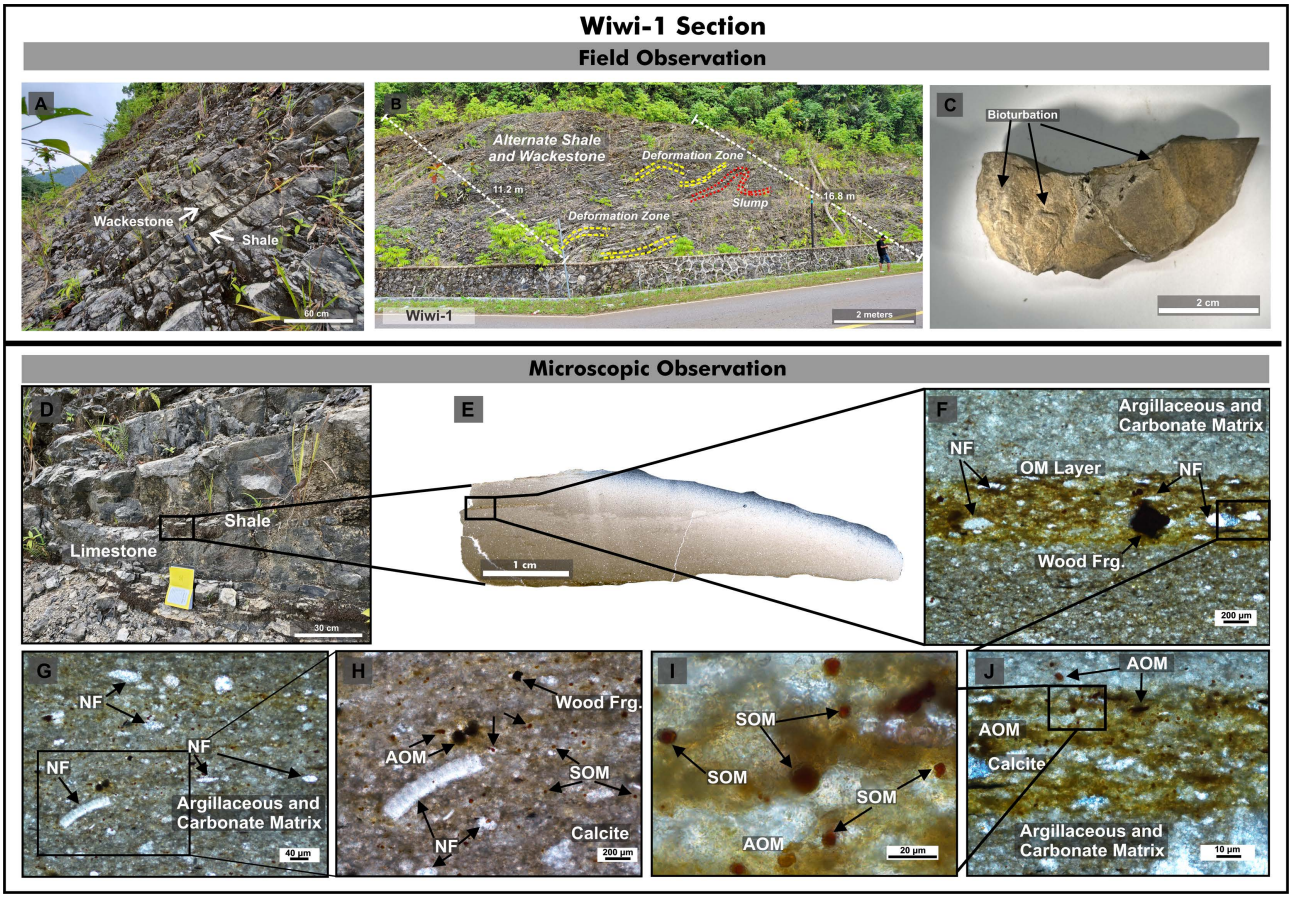

Figure 4. Field and microscopic observations in section Wiwi-1. (A)-(D) Alternating shale and limestone in the Tokala Formation, with observed bioturbation. (E) Detailed observation of a Wiwi-1 sample. (F), (G) Organic matter (OM) detected as a thin layer in argillaceous and carbonate matrix, with wood fragments and foraminifera. (I), (J) Dispersed structured organic matter (SOM) and neomorphic foraminifera (NF).

The bioturbation intensity within this interval was relatively poorly developed. Organic matter such as AOM tended to be more abundant, with both dispersed and laminar distributions (Figures 5(H)-(L)). Framboidal pyrite was common and poorly sorted within the shale facies, predominantly composed of large framboids (10.7 - 17.5 μm), followed by moderately sized framboids (6 - 9 μm; Figure 6). We assigned this shale as weakly laminated shale (WLS) facies. Although the shale layers emitted an oily odor, no oil stains were visible during macroscopic or microscopic observation. The limestone layers transitioned into finer grains supported by matrix, in which no skeletal fragments were observed. Therefore, limestone in this section was assigned as lime mudstone (LM) facies. Further north, another Tokala Formation interval was observed as 23-m-thick outcrops with good stratification of limestone and shale layers of equal thickness in the Bule-1 and Bule-2 sections (Tokala Formation; Figure 3). The shale layers showed similar characteristics to all of the abovementioned sections; however, skeletal fragments were suspended between argillaceous matrix and organic-rich layers (Figure 6(G), Figure 6(I), Figure 6(J)).

The bioturbation intensity within this interval was relatively poorly developed. Organic matter such as AOM tended to be more abundant, with both dispersed

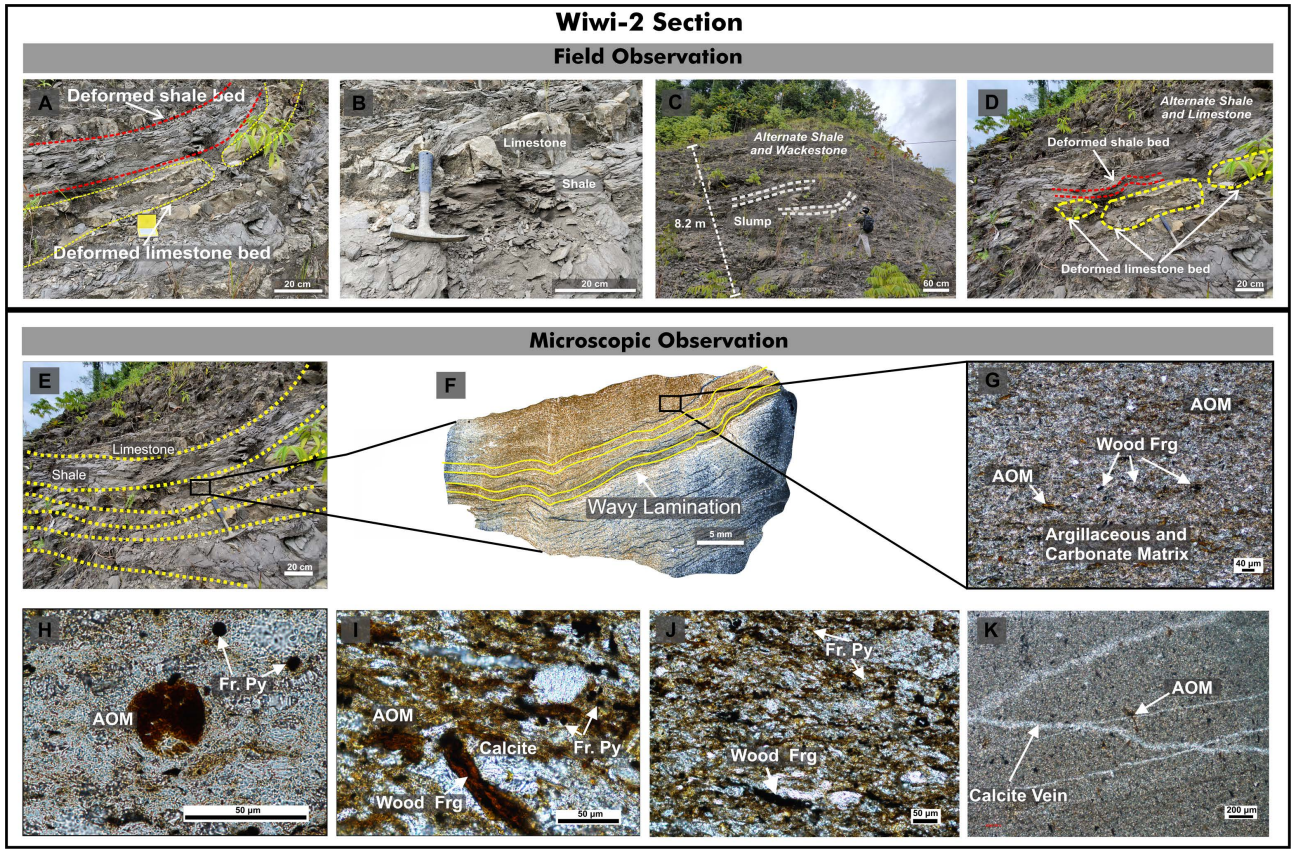

Figure 5. Tokala Formation outcrop in section Wiwi-2. (A)-(D) Alternating gray shale and limestone, with deformation features. (E)-(G) Observation area for field to microscopic observations. (G) Dispersed amorphous organic matter (AOM) with wood fragments in argillaceous and carbonate matrix. (H)-(J) Framboidal pyrites depicted with AOM and weakly laminated OM. (L) Fractures in a limestone sample.

and laminar distributions (Figures 5(H)-(L)). Framboidal pyrite was common and poorly sorted within the shale facies, predominantly composed of large framboids (10.7 - 17.5 μm), followed by moderately sized framboids (6 - 9 μm; Figure 5). We assigned this shale as weakly laminated shale (WLS) facies (Figure 5). Although the shale layers emitted an oily odor, no oil stains were visible during macroscopic or microscopic observation. The limestone layers transitioned into finer grains supported by matrix, in which no skeletal fragments were observed. Therefore, limestone in this section was assigned as lime mudstone (LM) facies.

Further north, another Tokala Formation interval was observed as 23-m-thick outcrops with good stratification of limestone and shale layers of equal thickness in the Bule-1 and Bule-2 sections (Tokala Formation; Figure 3). The shale layers showed similar characteristics to all of the abovementioned sections; however, skeletal fragments were suspended between argillaceous matrix and organic-rich layers (Figure 6(G), Figure 6(I), Figure 6(J)). The bioturbation intensity within

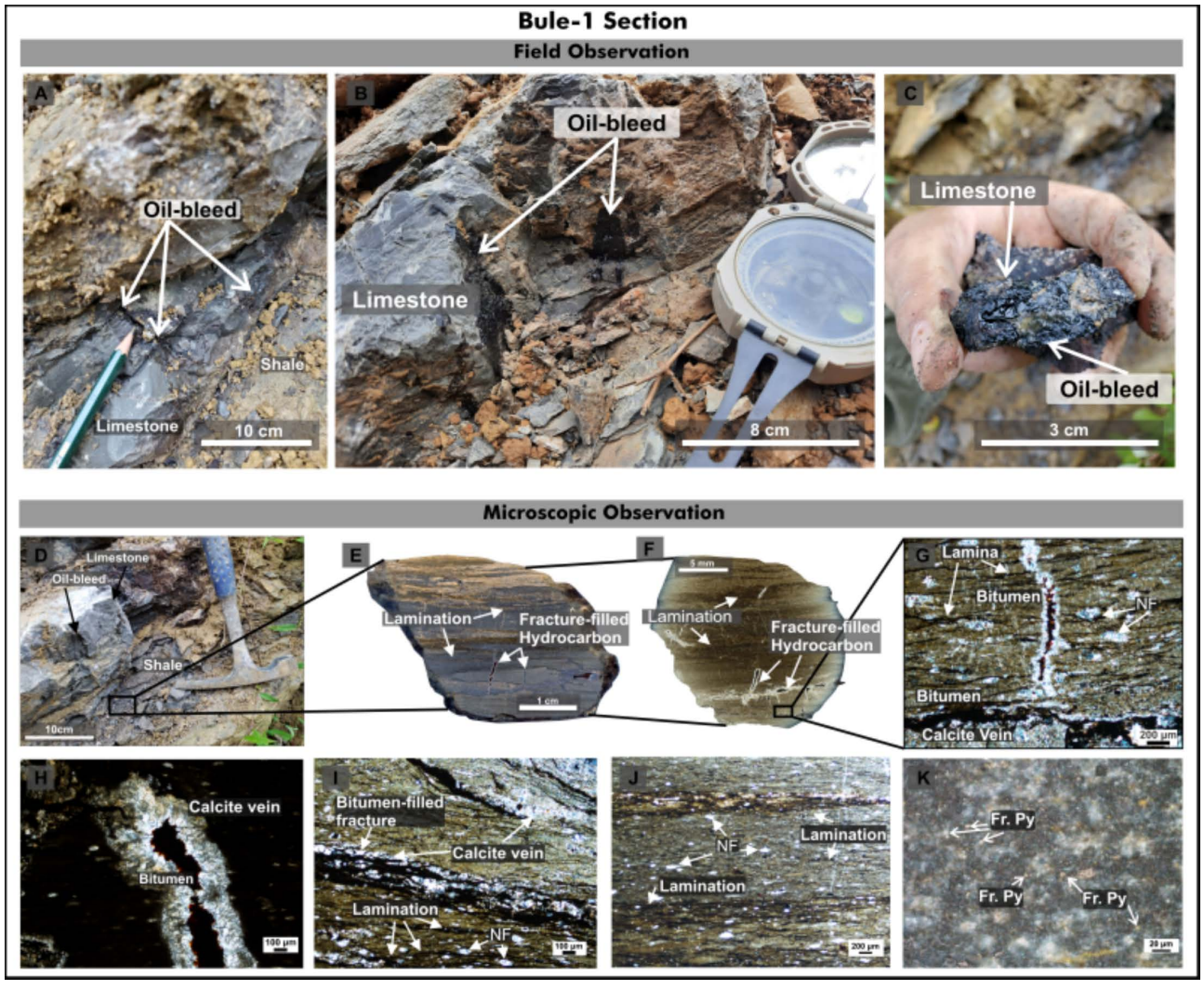

Figure 6. Outcrop of the Tokala Formation in section Bule-1. (A)-(D) Alternating shale and limestone, and oil bleed observed within the fractures of limestone intervals. (E), (F) Lamination structure and micro-scale fracture-filled bitumen. (G), (H) Laminated OM, intersected by fractures filled with bitumen. (I)-(K) NF submerged in argillaceous and carbonate matrix.

this interval was also poorly developed, while organic matter such as AOM tended to be more abundant in laminar distributions (Figure 6(G), Figure 6(I), Figure 6(J)). Framboidal pyrite was common and poorly sorted within the shale facies, predominantly composed of large framboids (10.7 - 17.5 μm).

4.2. Major Element Compositions

In general, SiO_2, Al_2O_3, and CaO were the predominant major oxides in our samples, depending on the lithology. Therefore, we describe the composition of major oxides, and provide our analysis of other oxides in Supplementary Data 1A. The shale lithofacies traversed in this research area generally showed varied elemental concentrations. MBCAS facies had 24.06% - 24.11% SiO_2 content, 10.33% - 10.55% Al_2O_3 content, and 28.66% - 28.72% CaO content; WLACS facies exhibited 35.60% - 36.60% SiO_2 content, 14.15% - 14.75% Al_2O_3 content, and 17.61% - 34% CaO content; and SLCAS facies exhibited 19.50% - 23.66% SiO_2 content, 4.34% - 7.27% Al_2O_3 content, and 36.11% - 51% CaO content. Furthermore, FW and LM facies were characterized by high CaO content (47.71% - 53.05%), low SiO_2 content (3.45% - 8.74%), and extremely low Al_2O_3 content (0.24% - 0.81%). Strong correlations were observed among each oxide, particularly the three dominant oxides. Al_2O_3 content was positively correlated with SiO_2 and K_2O content and negatively correlated with CaO content (Figure 7). CaO content was negatively correlated with both SiO_2 and MgO content (Figure 7). These relationships may be related to mineralogical content and could potentially be applied for petrochemical discrimination.

4.3. Bulk Organic Geochemical Characteristics

The bulk organic geochemistry of all lithofacies in this research tended to be rich in TOC and had high potential yield (PY). Specifically, the MBCAS and WLACS facies showed high TOC values, ranging from 1.20% to 1.28% and 3.9% to 4.0%, respectively, with corresponding PY values ranging from 2.10 to 2.24 and from 6.14 to 20.91, respectively (Supplementary Data 1C). Hydrogen index (HI) and S2 values were also high in the MBCAS (176 - 182 mg HC/g and 2.03 - 2.06 mg/g, respectively) and WLACS (447 - 500 mg HC/g and 17.42 - 20.24 mg/g, respectively) facies. In contrast, oxygen index (OI) and S3 values tended to be slightly lower in the MBCAS facies, ranging as 54 - 62 and 0.28 - 0.35 mg CO_2/g, respectively, and extremely low in the WLACS facies, ranging as 7 - 11 and 0.30 - 0.36 mg CO_2/g, respectively.

Similarly, the SLCAS facies had high TOC content (2.07% - 2.56%) and PY (7.40 - 13.24). HI values ranged from 384 to 472 mg HC/g in SLCAS facies, and S2 values were high (7.3 - 13.13 mg HC/g). S3 and OI showed low values, at 0.60 - 0.75 mg CO_2/g and 24 - 36 mg HC/g, respectively. Organic matter in the source rock of all lithofacies exhibited early thermal maturity, with Tmax values of 436˚C - 437˚C for MBCAS, 434˚C - 436˚C for WLACS, and 434˚C - 437˚C for SLCAS. Our geochemical characterization of the limestone facies FW and LM

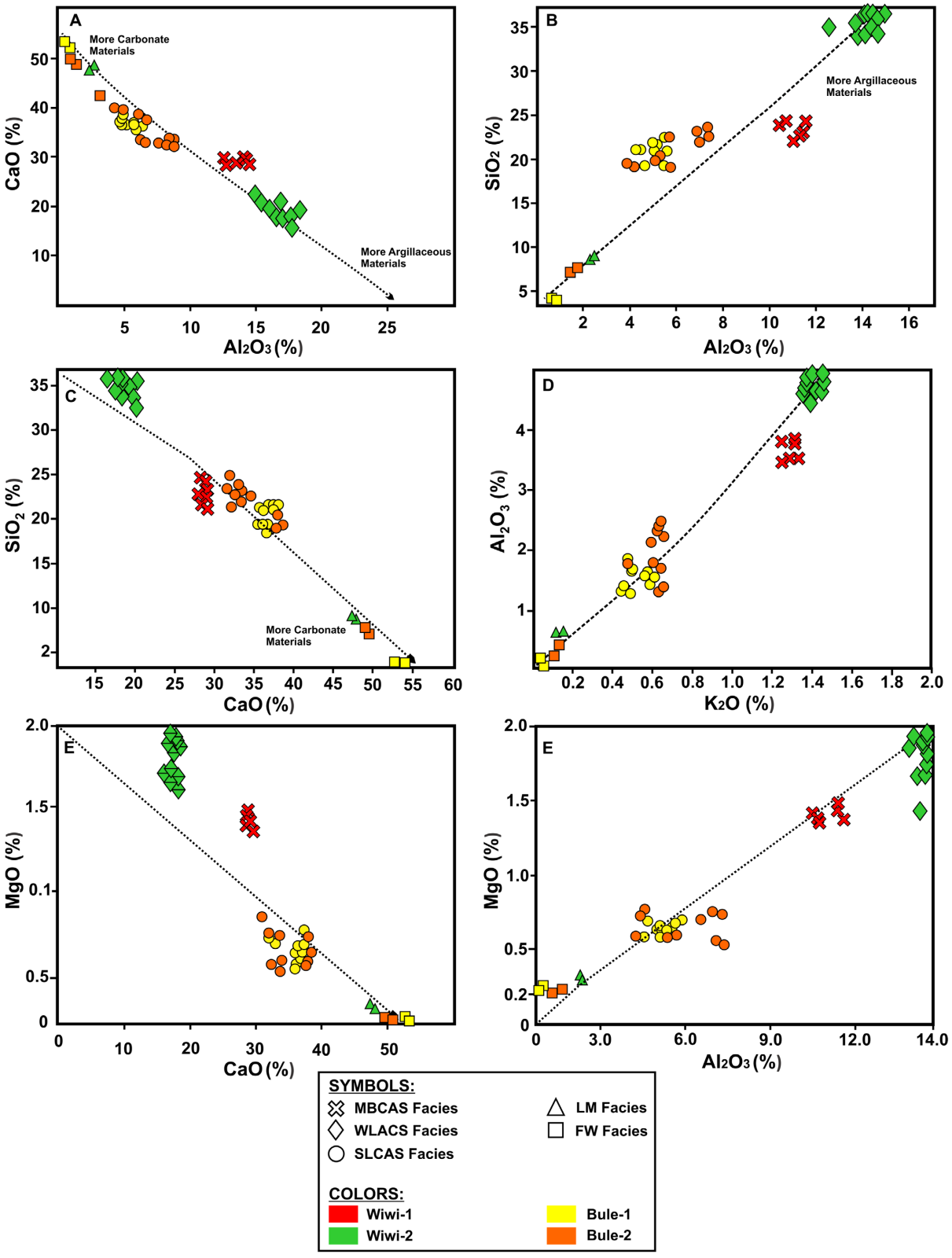

Figure 7. Correlation plots generated to determine the relationships between compounds from each lithofacies, including massive bioturbated calcareous-argillaceous shale (MBCAS), weakly laminated argillaceous-calcareous shale (WLACS), strongly laminated calcareous-argillaceous shale (SLCAS), and two limestones: lime mudstone (LM) and foraminifera wackestone (FW).

showed low to moderate TOC content. Specifically, TOC content ranged as 0.56 - 0.79 wt.% for FW and 0.29 - 0.33 wt.% for LM, corresponding to low to moderate PY values (0.10 - 3.64 and 0.77 - 0.80, respectively). These facies had significant HI values of 90 - 449 and 229 - 230 mg HC/g, respectively. S2 values were low, ranging as 0.09 - 3.55 for FW facies and 0.75 - 0.76 for LM facies. OI and S3 values ranged as 41 - 54 and 0.21 - 0.32 mg CO_2/g, respectively, in the FW facies and 81 - 88 and 0.28 - 0.29 mg CO_2/g, respectively, in the LM facies (as shown in detail in Supplementary Data 1B), indicating significant concentrations in these facies.

5. Discussion

5.1. Petrochemistry of The Tokala Formation: Lithofacies Complexity

A problem arose when our lithofacies discrimination method was applied to the multiple shale layers found in every section. Rock described as massive mudstone in the field could be massive, weakly, or strongly laminated mudstone according to our thin section observations. As it would be impossible to prepare thin sections from all shale layers, we turned to quantitative petrochemical classification. The content of three major constituents is commonly used for mudstone and shale classification: quartz, carbonates, and clay minerals [31]-[33], with their content typically determined by XRD analysis. Not specific only for shale and mudstone, the determination mineralogical composition obtained from XRD analysis even also commonly used for soil or slag [34]. As quantitative mineralogical data were not available, the content of major elements determined by XRF analysis was used in this study (Supplementary Data 1A). This type of classification approach has been applied in previous studies [35] for example, proposed chemical discrimination for sedimentary rocks, dividing shale into "shale" and "Fe-shale," and interpreting relative Al_2O_3 content as being related to grain size [36]. In the present study, all samples were initially classified as mudstone (sensu stricto) or shale, when fissility was observed. Therefore, we applied a direct classification scheme based on the content of the three major shale components [31]-[33], in which quartz, carbonate, and clay minerals are represented by SiO_2, CaO, and Al_2O_3, respectively. This approach is justified by the correlations detected among these compounds. Our samples showed a positive correlation between SiO_2 and Al_2O_3. In some cases, increased SiO_2 content was followed by decreased Al_2O_3 content due to fluctuation between biogenic and detrital inputs [37]. Given the observed positive correlation, these oxides were interpreted as being related solely to either detrital fractions or argillaceous materials (aluminosilicates). The fluctuation between biogenic and detrital inputs was further shown by the negative correlations of CaO with SiO_2 and Al_2O_3, as increasing carbonate proportions were associated with reduced proportions of argillaceous and siliceous minerals (**Figure 8**).

In regard to that, our classification scheme distinguished three groups,

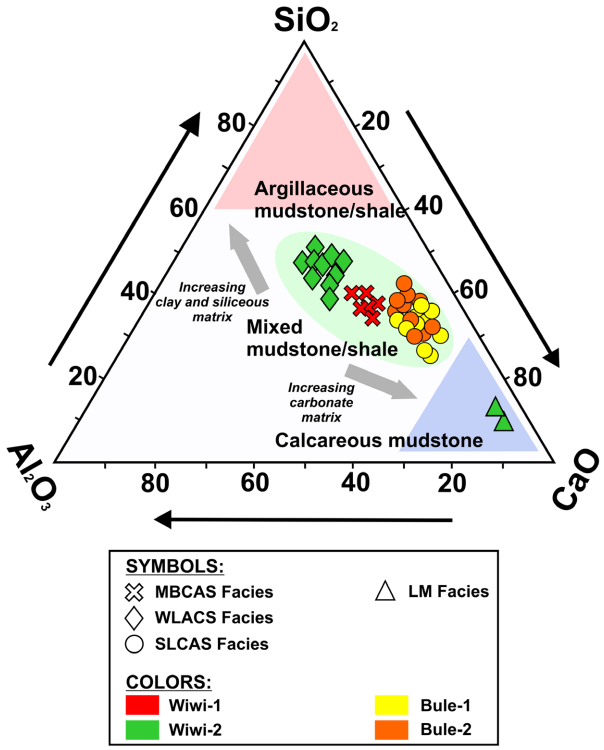

Figure 8. Proposed shale and mudstone classification system based on the content major shale mineralogical constituents: quartz, carbonates, and clay minerals [31]-[33].

argillaceous, "mixed," and calcareous shales (**Figure 8**), where the term "mixed" pertains to the balance among the three major components (CaO, SiO_2, and Al_2O_3), resulting in classifications such as argillaceous-calcareous (ar-ca) and calcareous-argillaceous (ca-ar), which are terms adapted from [38].

In regard to that, he petrochemistry further discriminated the observed lithofacies, resulting in the differentiation of samples into distinct clusters. For example, the WLS facies exemplified the ar-ca group, which was typified by WLACS from the Wiwi-2 section, whereas the MBS and SLS facies further represented the ca-ar group, which was typified by MBCAS facies from the Wiwi-1 section and SLCAS facies from the Bule-1 and Bule-2 sections. The SLCAS facies had higher CaO content, indirectly suggesting higher carbonate content compared to other shale facies. The WLACS facies had the highest SiO_2 and Al_2O_3 content, which may be related to high argillaceous input. The MBCAS facies showed similar proportions of SiO_2, Al_2O_3, and CaO (**Figure 8**). This balance between carbonate and argillaceous content (CaO-SiO_2) may have been related to the deposition energy, with higher carbonate levels correlated with more stable energy [39] [40] and higher argillaceous content related to more sediment supply due to high energy, perhaps associated with the supply of detritus materials from the land (**Figure 8**).

5.2. Source Rock Characteristics: Maturity, Quantity, and Quality

The source rock maturation process can significantly reduce TOC content and

S2 values [41]-[43]. Therefore, these parameters do not represent initial organic matter conditions, and thermal maturity information is required prior to further geochemical characterization. According to our data, all facies had mostly reached the early mature stage (T_{max}: 435˚C - 437˚C), with some samples still in the immature stage [T_{max} < 435˚C; 37]. This thermal stage is the best condition for understanding source rock characteristics, as the organic matter has not been altered by maturation and still represents initial syn-depositional conditions.

The geochemical characterization of source rock has been conducted on several Mesozoic shales, including Tokala Formation, within neighboring basin of our research area, Tomori Basin [18] exhibiting 0.32 - 3.46 wt.% of TOC. These data aligned with the all of our shale facies (MBCAS, WLACS, SLCAS) which also show high value of TOC in range from 1.20 - 4.0 wt.%. This similarity indicates that the Tokala Formation from Tomori Basin and from our research area in southern Sulawesi represent potential source rock characteristics in the term of quantity organic matter.

In this research, we adopted a common source rock classification [44]. The carbonate-dominated facies (CaO > 50%), particularly the LM and FW facies, are considered carbonate-poor, as indicated by their low TOC and S2 levels (**Figure 9(A)**). The shale facies tended to have higher levels of organic matter, increasing in the order MBCAS (good) < SLCAS (good to very good) < WLACS (very good to excellent) (**Figure 9(A)**).

Furthermore, in terms of the quality of organic matter, all of our facies tended to be composed of type II kerogen (**Figure 9(B)**) with HI increasing in the order FW < MBCAS < LM < SLCAS < WLACS. This HI trend may be related to the amount of hydrogen-rich organic material, either based on the original organic matter or excellent preservation of organic matter in the sediments [43].

5.3. Lithological, Mineralogical, and Petrochemical Perspectives on Source Rocks

All shales in the research area tended to have higher organic matter content than "true carbonate" (CaO > 50%) intervals. This phenomenon diverged slightly from the definition of carbonate source rock as organic-rich sedimentary rock comprised of at least 50% carbonate minerals, but also corresponds to layers containing less than 50% carbonate but with substantial amounts of marl [39]. Although two important geological scenarios for organic matter enrichment in carbonate rocks have been highlighted [45]., *i.e.*, high primary productivity and elevated organic preservation, we believe that organic matter enrichment and other source rock characteristics are closely related to lithological, mineralogical, and petrochemical aspects of the rock. For example, the defined carbonate source rock [39] appears to be composed of a mixture of carbonate and argillaceous materials, which is a mineralogical matter regardless of depositional and enrichment processes.

The clearest distinction between poor and good source rocks was observed from petrochemical and mineralogical perspectives, in terms of the inverse

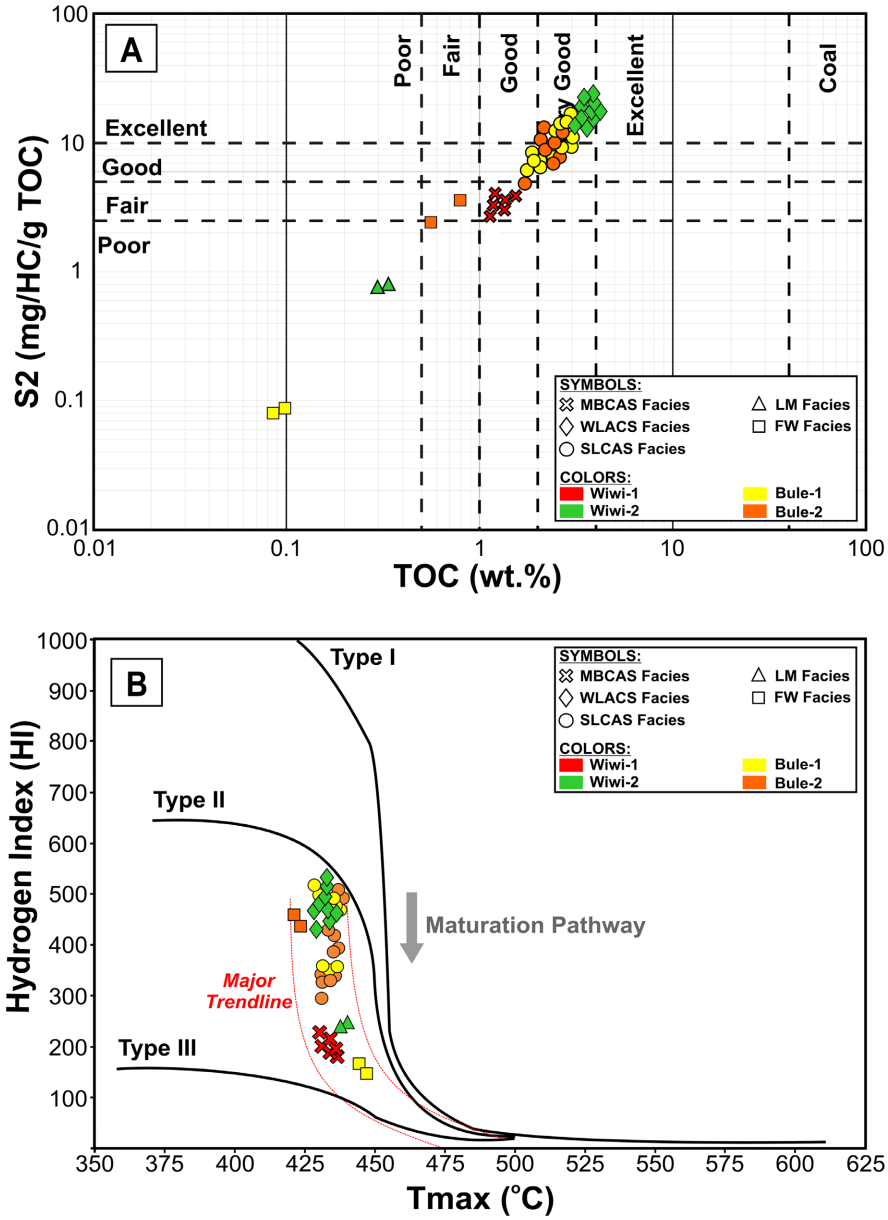

Figure 9. Organic matter quantity, represented by total organic carbon (TOC) content and S_2 values, and organic matter quality, inferred from a pseudo-van Krevelen diagram [after [42], [44]]. This geochemical characterization indicated that shale facies are tend to more promising compared to the limestone facies based on quantity and quality of organic matter.

relationship of CaO-SiO_2 and Al_2O_3 ratios. Increasing carbonate content was followed by slight decreases in TOC content and PY (Figure 10). Moreover, high siliciclastic material input was negatively correlated with source rock quantity and quality (TOC, PY, and HI). Therefore, the quantity and quality of carbonate source rock are functions of carbonate and siliciclastic content, which are linked to sedimentation processes. Slow carbonate accumulation results in poor organic matter preservation, leading to the degradation of organic matter. Moreover, rapid siliciclastic transportation and sedimentation during mudstone deposition

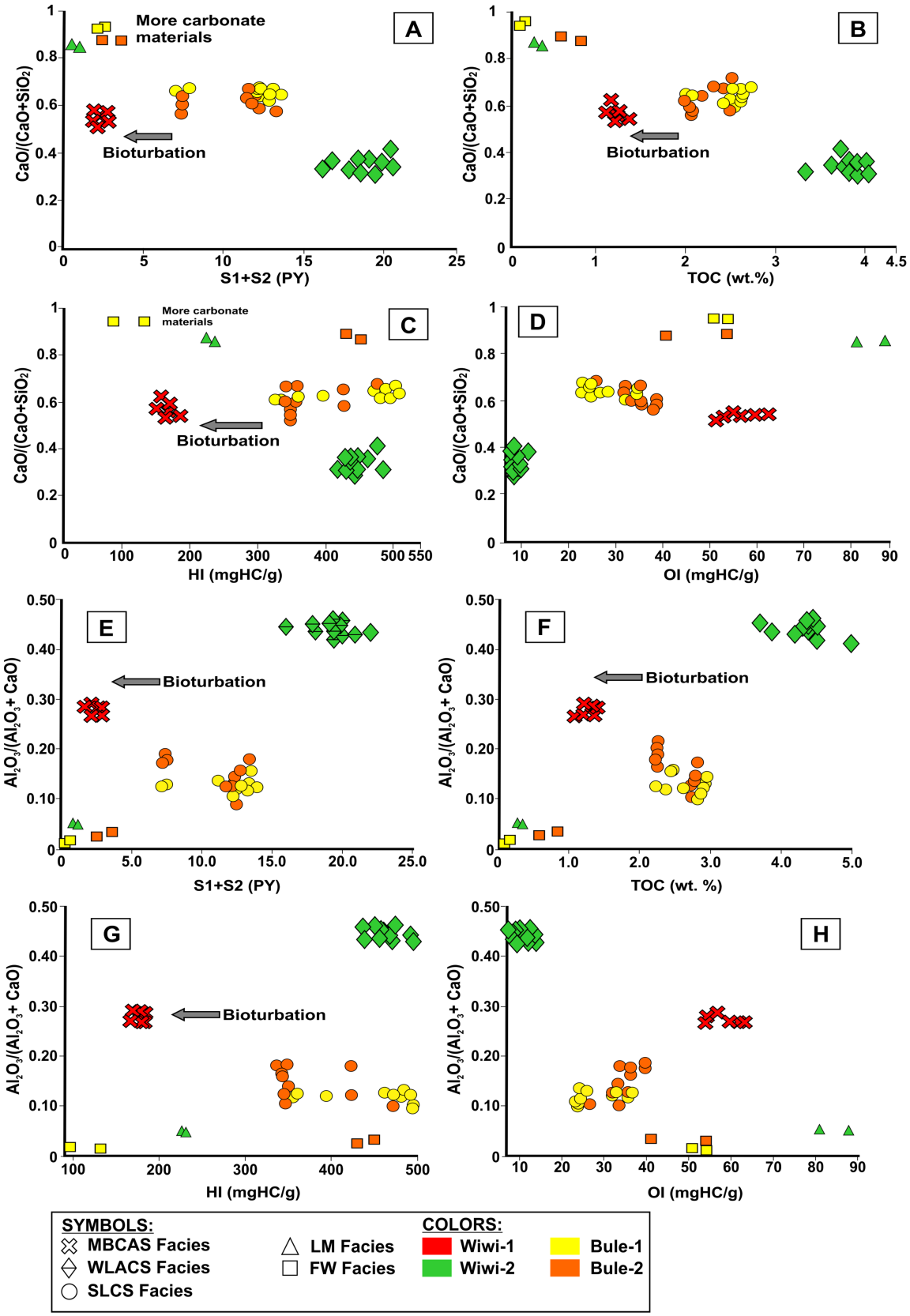

Figure 10. Bivariate plots of CaO/(CaO + SiO_2) representing the carbonate-siliciclastic ratio, and extended to sedimentation processes vs. (A) potential yield (PY), (B) TOC, (C) HI, and (D) oxygen index (OI).

can dilute the OM concentration with high clay input [43]-[46].

Not restricted to sedimentation processes, the presence of argillaceous content is also important for the formation of carbonate source rock, as clay minerals can adsorb organic matter [47]-[49]. To explain the possibility of clay adsorption, we utilize Al_2O_3 as a representative clay mineral. Positive correlations were observed between Al_2O_3 and PY, TOC, and HI values (**Figures 10(E)-(G)**), suggesting that clay minerals influenced the organic matter enrichment [49] [50], in particular within the source rock, as demonstrated in our study. Therefore, the occurrence of clay minerals in the depositional environment should be considered along with organic preservation and productivity [45].

Another interesting observation is that MBCAS facies trends were always shifted, such that increases in Al_2O_3 were not followed by corresponding increases in TOC, PY, and HI. Such conditions could potentially be influenced by macro-scale factors other than mineralogical and petrochemical factors.

The decreases in TOC content, PY, and HI, even with decreasing CaO and increasing Al_2O_3 content, in MBCAS facies may have been related to bioturbation. Bioturbation causes organic matter destruction, and therefore significantly influences organism activity and oxic conditions [43]. Organism activity can destroy accumulated organic matter (as food), and oxic conditions may affect organic matter degradation, as discussed in previous studies [e.g., [51] and [52]] where bioturbation was shown to have caused destruction of organic matter. With regard to laminated intervals, our SLCAS facies had high organic matter quantity and quality, which are also typical for carbonate source rock [39] [52] [53], and the WLACS facies showed excellent organic matter quality. Lamination indicates slow, stable deposition, which is suitable for organic matter preservation [39] [45]. Based on these factors, we summarized the lithological, mineralogical, and petrochemical characteristics associated with our facies variations to understand which facies are preferable as source rock and prospective horizons (**Figure 11**).

6. Conclusion

In this study, carbonate lithologies showed different organic matter (organofacies) characteristics, allowing us to divide carbonate rocks into two major groups: limestone (CaO > 50%) and shale (CaO < 15% - 50%). This shale group exhibited specific lithological and petrochemical characteristics in accordance with distinctive organic matter quantity and quality. The shale group was further divided into three subgroups with moderate to high organic matter content, including bioturbated (MBCAS), strongly laminated, and weakly laminated (WLACS and SLCAS) facies. These categories were taken to be related to the depositional processes, in which the counterbalance of CaO and SiO_2-Al_2O_3 may reflect depositional energy and organic matter preservation. Argillaceous materials play important roles in facilitating organic matter accumulation in source rock with carbonate affinity through clay mineral adsorption. Finally, the shale facies of

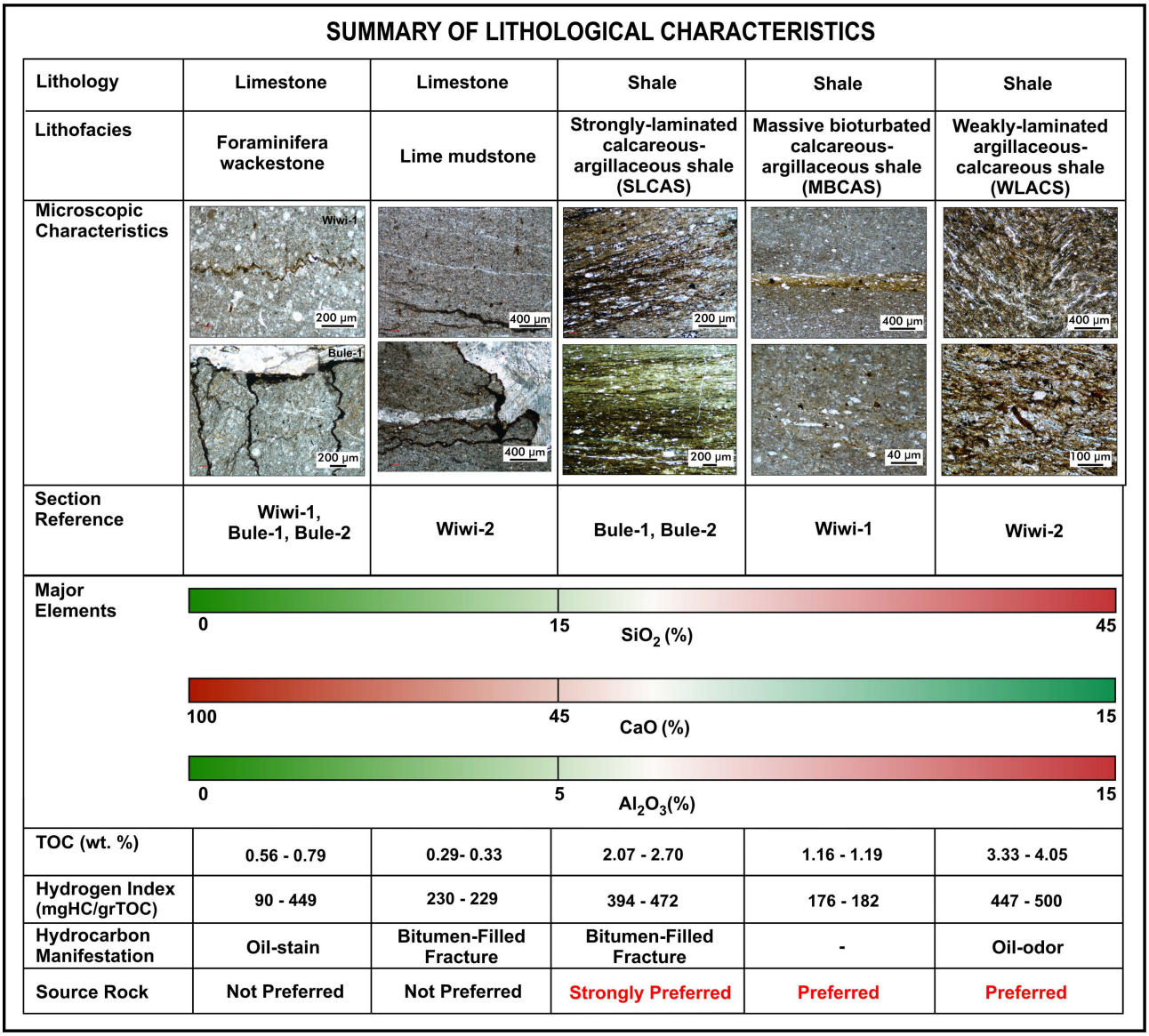

Figure 11. Summary of lithological characteristics, including microscopic characterization, inorganic (major compounds) and organic geochemistry. The moderate CaO group appears more likely to be good source rock, with considerable levels of SiO_2 and Al_2O_3 than the enriched CaO group.

Tokala Formation in southeastern Sulawesi represent prospective source rock horizons.

Acknowledgements

We thank Akita University for supporting our research activities, and express our gratitude to the Ministry of Education, Culture, Sports, Science, and Technology, Japan, for funding our research project. We are grateful to Hasanuddin University for providing research support. We express our gratitude to the late Professor Asri Jaya for discussion and critical comments, as well as Dr. Sc. Renaldi Suhendra, Dr. Sc. Paolo Martizzi, Mrs. Anggi Yusriani, Mr. Takumi Mimura, Mr. Rinaldi Ikhram, Dr. Sc. Muhammad Andriansyah Gurusinga, Mrs.

Lauti Dwita Santy, and Ms. Sam Sam Yonino Naita for laboratory work, discussion, and suggestions, and to Mr. Baso Rezki Maulana for fieldwork support.

Conflicts of Interest

The authors declare no conflicts of interest regarding the publication of this paper.

References

[1] Energy and Mineral Resources (2022) Indonesian Sedimentary Basin Map Based on Gravity and Geological Data.

[2] Bradshaw, C.J.A., Boutin, S. and Hebert, D.M. (1997) Effects of Petroleum Exploration on Woodland Caribou in Northeastern Alberta. *The Journal of Wildlife Management*, **61**, 1127-1133. https://doi.org/10.2307/3802110

[3] Livsey, A.R., Duxbury, N. and Richards, F. (1992) The Geochemistry of Tertiary and Pre-Tertiary Source Rocks and Associated Oils in Eastern Indonesia. *Proceedings of the* 21*st Annual Convention and Exhibition of Indonesian Petroleum Association*, 499-530. https://doi.org/10.29118/IPA.867.499.520

[4] Peters, K.E., Fraser, T.H., Amris, W., Rustanto, B. and Hermanto, E. (1999) Geochemistry of Crude Oils from Eastern Indonesia. *AAPG Bulletin*, **83**, 1927-1942. https://doi.org/10.1306/E4FD4643-1732-11D7-8645000102C1865D

[5] Noble, R., Orange, D., Decker, J., Teas, P. and Baillie, P. (2009) Oil and Gas in Deep Marine Sea Floor Cores as Indicator of Active Petroleum Systems in Indonesia. *Proceedings of the* 21*st Annual Convention and Exhibition of Indonesian Petroleum Association*. https://doi.org/10.29118/IPA.219.09.G.044

[6] Hartono, B.M., Subroto, E.A., Kesumajana, A.H.P., Andrianto, R., Malvinas, G. and Wahyudiono, J. (2023) Geochemistry of Carbonate-Derived Oils in the Seram Basin, Eastern Indonesia: A New Hydrocarbon Generation, Migration, and Preservation Model for Exploration in Fold-Thrust Belts. *Journal of Asian Earth Sciences*, **250**, Article 105647. https://doi.org/10.1016/j.jseaes.2023.105647

[7] Price, P.L., O'Sullivan, T. and Alexander, R. (1987) The Nature and Occurrence of Oils in Seram, Indonesia. *Proceeding of* 16*th Annual Convention of AAPG*, **1**, 141-173.

[8] Davidson, J.W. (1991) The Geology and Prospectivity of Buton Island, S.E. Sulawesi, Indonesia. *Proceedings of the* 20*th Annual Convention and Exhibition of Indonesian Petroleum Association*, Jakarta, 8-10 October 1991, 209-233.

[9] Satyana, A.H., Irawan, C. and Kurniawan, W. (2013) Revisit Geology and Geochemistry of Buton Asphalt Deposits, SE Sulawesi: Implications for Petroleum Exploration of Buton Area. *Proceedings of the* 37*th Annual Convention and Exhibition of Indonesian Petroleum Association*, Jakarta, 15-17 May 2013, 1-18.

[10] George, S.C., Lisk, M. and Eadington, P.J. (2004) Fluid Inclusion Evidence for an Early, Marine-Sourced Oil Charge Prior to Gas-Condensate Migration, Bayu-1, Timor Sea, Australia. *Marine and Petroleum Geology*, **21**, 1107-1128. https://doi.org/10.1016/j.marpetgeo.2004.07.001

[11] Phoa, R.S.K. and Samuel, L. (1986) Problem of Source Rock Identification in Salawati Basin, Irian Jaya. *Proceedings of the* 15*th Annual Convention of Indonesian Petroleum Association*, Jakarta, October 1986, 405-421.

[12] Ozza, T., Sompie, T., Silalahi, E., Utoro, E.S. and Miraza, D. (2019) Source Rock Maturity, Timing of Hydrocarbon Generation and Expulsion of the Arar and Walio

Areas, Salawati Basin, West Papua, Indonesia. *Proceedings of the* 43*rd Annual Convention of the Indonesian Petroleum Association*, Jakarta, 4-6 September 2019, 40-60.

[13] Dolan, P.J. and Hermany (1988) The Geology of the Wiriagar Field, Bintuni Basin, Irian Jaya. *Proceedings of* 17*th Annual Convention of Indonesian Petroleum Association*, Jakarta, October 1988, 53-87.

[14] Subroto, E. and Sapiie, B. (2014) Source Rocks Assessment in Bintuni Basin, Papua, Indonesia: The Answer! *Annual International Conference on Geological & Earth Sciences*, Singapore, 22-23 September 2014, 99-103.

[15] Satyana A.H. and Zaitun, S. (2016) Origins of Oils and Gases at Banggai Sula Microcontinent, Eastern Sulawesi North Moluccas: Constraints from Biomarkers and Isotope Geochemistry Implications for Further Exploration of Cenozoic and Pre-Cenozoic Objectives. *Proceedings of Indonesian Petroleum Association Fourteenth Annual Convention and Exhibition*, Jakarta, 25-27 May 2016, 1630-1656.

[16] Kurniawan, A.P., Mardianza, A., Firman, I. and Fajar, M. (2019) New Biomarker Evidences of Mesozoic Petroleum System in the Unexplored Tokala Area, Eastern Sulawesi. *Proceedings of the* 43*rd Annual Convention and Exhibition of Indonesian Petroleum Association*, Jakarta, 4-6 September 2019, 2173-2186.

[17] Burhanuddin, M.S., Subroto, E.A., Santy, L.D., Susanto, V. and Fahruddin, A. (2020) Geochemistry Characterization of Oil and Source Rock in Southern Tomori Basin. *The* 5*th International Conference of Geology*, 16-17 November 2020, 23-24.

[18] Santy, L.D. (2016) The Mesozoic Source Rock Identification in Tomori Basin, East Arm of Sulawesi and Its Implication for Petroleum Play. *Proceedings of Indonesian Petroleum Association. Technical Symposium*, Jakarta, 25-27 May 2016, 1-19.

[19] Surono (1994) Stratigraphy of the SE Sulawesi Continental Terrane, Eastern Indonesia. *Journal of Geology and Mineral Resource*, **31**, 4-10.

[20] Surono and Hartono, U. (2013) Geology of Sulawesi. Centre of Geological Survey, Ministry of Mineral and Energy Resources of Indonesia. LIPI Press.

[21] Rusmana, E., Sukido, Sukarna, D., Haryanto, E. and Simandjuntak, T.O. (1993) Geological Map of the Lasusua Kendari Quadrangles (Quadrangles 2112, 2212), Sulawesi, Scale 1:250,000.

[22] Nugraha, A.M.S. and Hall, R. (2022) Neogene Sediment Provenance and Paleogeography of SE Sulawesi, Indonesia. *Basin Research*, **34**, 1714-1730. https://doi.org/10.1111/bre.12682

[23] Spakman, W. and Hall, R. (2010) Surface Deformation and Slab-Mantle Interaction during Banda Arc Subduction Rollback. *Nature Geoscience*, **3**, 562-566. https://doi.org/10.1038/ngeo917

[24] Advokaat, E.L. and van Hinsbergen, D.J.J. (2023) Finding Argoland: Reconstructing a Microcontinental Archipelago from the SE Asian Accretionary Orogen. *Gondwana Research*, **128**, 161-263. https://doi.org/10.1016/j.gr.2023.10.005

[25] Villeneuve, M., Cornée, J.J., Gunawan, W., Martini, R., Tronchetti, G., Janin, M.C., Saint Marc, P. and Zaninetti, L. (2001) La succession lithostratigraphique du bloc de Banda dans la region de Kolonodale (Sulawesi Central, Indonesie). *Bulletin de la Société géologique de France*, **172**, 59-68. https://doi.org/10.2113/172.1.59

[26] Audley-Charles, M.G., Carter, D.J., Barber, A.J., Norvick, M.S. and Tjokrosapoetro, S. (1979) Reinterpretation of the Geology of Seram: Implications for the Banda Arcs and Northern Australia. *Journal Geological Society of London*, **136**, 547-568. https://doi.org/10.1144/gsjgs.136.5.0547

[27] Kemp, G. and Mogg. W. (1992) A Re-Appraisal of the Geology, Tectonics, and Prospectivity of Seram Island, Eastern Indonesia. *Proceedings of Indonesian Petro-*

leum Association. Twenty First Annual Convention, Jakarta, October 1992, 521-552.

[28] Nugraha, A.M.S. and Hall, R. (2022) Neogene Sediment Provenance and Paleogeography of Se Sulawesi, Indonesia. *Basin Research*, **34**, 1714-1730. https://doi.org/10.1111/bre.12682

[29] Simmons, K. (2023) Standard Operating Procedure (SOP) for Sediment Sampling.

[30] Takahashi, G. (2015) Sample Preparation for X-Ray Fluorescence Analysis III: Pressed and Loose Powder Methods. *The Rigaku Journal*, **31**, 26-30.

[31] Ulmer-Scholle, D.S., Scholle, P.A., Schieber, J. and Raine, R.J. (2015). A Color Guide to the Petrography of Sandstones, Siltstones, Shales and Associated Rocks. American Association of Petroleum Geologists. https://doi.org/10.1306/m1091304

[32] Rojas, L.F., Quintero, P.Y. and Carrillo, Z.H. (2016) Brittleness Analysis: A Methodology to Identify Sweet Spots in Shale Gas Reservoirs.

[33] Mews, K.S., Alhubail, M.M. and Barati, R.G. (2019) A Review of Brittleness Index Correlations for Unconventional Tight and Ultra-Tight Reservoirs. *Geosciences*, **9**, Article 319. https://doi.org/10.3390/geosciences9070319

[34] Tangahu, B.V., Warmadewanthi, I., Saptarini, D., Pudjiastuti, L., Tardan, M.A.M. and Luqman, A. (2015) Ferronickel Slag Performance from Reclamation Area in Pomalaa, Southeast Sulawesi, Indonesia. *Advances in Chemical Engineering and Science*, **5**, 408-412. https://doi.org/10.4236/aces.2015.53041

[35] Herron, M. (1998) Geochemical Classification of Terrigenous Sands and Shales from Core or Log Data. *Journal of Sedimentary Research*, **58**, 820-829.

[36] Sprague, R.A., Melvin, J.A., Conradi, F.G., Pearce, T.J., Dix, M.A., Hill, S.D. and Canham, H. (2009) Integration of Core-Based Chemostratigraphy and Petrography of the Devonian Jauf Sandstones, Uthmaniya Area, Ghawar Field, Eastern Saudi Arabia.

[37] Martizzi, P., Chiyonobu, S., Hibi, Y., Yamato, H. and Arato, H. (2021) Middle-Late Miocene Paleoenvironment of the Japan Sea Inferred by Sedimentological and Geochemical Characterization of Coeval Sedimentary Rocks. *Marine and Petroleum Geology*, **128**, Article 105059. https://doi.org/10.1016/j.marpetgeo.2021.105059

[38] Lazar, O.R., Bohacs, K.M., Schieber, J., Macquaker, J.H.S. and Demko, T.M. (2022) 2 Mudstone Nomenclature. The American Association of Petroleum Geologists and Brazilpetrostudies. https://doi.org/10.1306/137122973860

[39] Palacas, J.G., Anders, D.E. and King, J.D. (1984) South Florida Basin—A Prime Example of Carbonate Source Rocks of Petroleum. American Association of Petroleum Geologists. https://doi.org/10.1306/st18443c6

[40] Xia, L.W., Cao, J., Wang, M., Mi, J.L. and Wang, T.T. (2019) A review of Carbonates as Hydrocarbon Source Rocks: Basic Geochemistry and Oil-Gas Generation. *Petroleum Science*, **16**, 713-728.

[41] Jarvie, D.M. (2012) Shale Resource Systems for Oil and Gas: Part 1—Shale Gas Resource Systems. In: Breyer, J.A., Ed., *Shale Reservoirs—Giant Resources for the* 21st *century*, American Association of Petroleum Geologists, 69-87.

[42] Dembicki, H. (2009) Three Common Source Rock Evaluation Errors Made by Geologists during Prospect or Play Appraisals. *AAPG Bulletin*, **93**, 341-356. https://doi.org/10.1306/10230808076

[43] Dembicki, Jr. (2017) Practical Petroleum Geochemistry for Exploration and Production, Elsevier, 217-252. https://doi.org/10.1016/b978-0-12-803350-0.00006-4

[44] Peters, K.E. and Cassa, M.R. (1994) Applied Source Rock Geochemistry—The Petroleum System from Source to Trap, 93-120. In: Magoon, L.B., Dow, W.G., Eds.,

The Petroleum System from Source to Trap, American Association of Petroleum Geologists.

[45] Harris, P.M. and Katz, B.J. (2005) Carbonate Mud and Carbonate Source Rocks. *Proceedings Abstract of* 2005 *Annual Convention of AAPG*, Calgary, 16-19 June 2005, 1.

[46] Tissot, B. and Welte, D.H. (1984) Petroleum Formation and Occurrence. 2nd Edition, Springer.

[47] Cordell, R.J. (1992) Carbonates as Hydrocarbon Source Rocks. *Developments in Petroleum Science*, **30**, 271-329. https://doi.org/10.1016/s0376-7361(09)70128-1

[48] Cao, Z., Jiang, H., Zeng, J., Saibi, H., Lu, T., Xie, X., *et al.* (2021) Nanoscale Liquid Hydrocarbon Adsorption on Clay Minerals: A Molecular Dynamics Simulation of Shale Oils. *Chemical Engineering Journal*, **420**, Article 127578. https://doi.org/10.1016/j.cej.2020.127578

[49] Zhao, T., Xu, S. and Hao, F. (2023) Differential Adsorption of Clay Minerals: Implications for Organic Matter Enrichment. *Earth*-Science Reviews, **246**, Article 104598. https://doi.org/10.1016/j.earscirev.2023.104598

[50] Yang, G., Zeng, J., Qiao, J., Liu, Y., Cao, W., Wang, C., *et al.* (2022) Differences between Laminated and Massive Shales in the Permian Lucaogou Formation: Insights into the Paleoenvironment, Petrology, Organic Matter, and Microstructure. *ACS Earth and Space Chemistry*, **6**, 2530-2551. https://doi.org/10.1021/acsearthspacechem.2c00245

[51] Demaison, G. and Bourgeois, F.T. (1984) Environment of Deposition of Middle Miocene (Alcanar) Carbonate Source Beds, Casablanca Field, Tarragona Basin, Offshore Spain. American Association of Petroleum Geologists. https://doi.org/10.1306/st18443c11

[52] Yurchenko, I.A., Moldowan, J.M., Peters, K.E., Magoon, L.B. and Graham, S.A. (2018) Source Rock Heterogeneity and Migrated Hydrocarbons in the Triassic Shublik Formation and Their Implication for Unconventional Resource Evaluation in Arctic Alaska. *Marine and Petroleum Geology*, **92**, 932-952. https://doi.org/10.1016/j.marpetgeo.2018.03.033

[53] Oehler, J.H. (1984) Carbonate Source Rocks in the Jurassic Smackover Trend of Mississippi, Alabama, and Florida. American Association of Petroleum Geologists. https://doi.org/10.1306/st18443c5